Cell, Vol. 117, 649–662, May 28, 2004, Copyright ©2004 by Cell Press

RNA and RNA Binding Proteins Participate in Early Stages of Cell Spreading through Spreading Initiation Centers

Carmen L. de Hoog,[1,2] Leonard J. Foster,[1,2] and Matthias Mann[1,*]
[1]Center for Experimental BioInformatics (CEBI)
Department of Biochemistry and Molecular Biology
University of Southern Denmark
Campusvej 55, DK-5230 Odense M
Denmark

Summary

Focal adhesions are specialized attachment and signaling centers that form at sites of cell-matrix contacts. We employed a quantitative mass spectrometry-based method called SILAC to identify and quantify proteins interacting in an attachment-dependent manner with focal adhesion proteins. Subsequent confocal microscopy revealed a previously undescribed structure, which we have termed a spreading initiation center (SIC), existing only in early stages of cell spreading. SICs contain focal adhesion markers, appear to be surrounded by an actin sheath, and, surprisingly, contain numerous RNA binding proteins, ribosomal RNA, and perhaps other RNAs. Interfering with the function of FUS/TLS, hnRNP K, and hnRNP E1 results in increased spreading. Spreading initiation centers are ribonucleoprotein complexes distinct from focal adhesions and demonstrate a role for RNA and RNA binding proteins in the initiation of cell spreading.

Introduction

The adhesion of a cell to a substrate is necessary to allow cells to spread and migrate. Studies in the 1970s demonstrated that cells do not attach uniformly to a surface but that they do so through specialized structures called focal adhesions. These cell-matrix attachments play an essential role in many vital cellular processes, including motility, proliferation, differentiation, regulation of gene expression, and survival (Sastry and Burridge, 2000). The ability of cells to adhere to the extracellular matrix is an important determinant of cytoskeletal organization and thereby also of morphology (Murphy-Ullrich, 2001). Modulation of adhesion is important in many cellular or tissue responses: tissue remodeling during development, wound healing, and also tumor cell metastasis depends on cancerous cells being able to release from the basal membrane (Turner et al., 2001). Migration is diminished in cells that are strongly attached with abundant stress fibers and focal adhesions (Huttenlocher et al., 1996). The characterization of the molecular constituents of these adhesions and their precise organization is important if we are to understand the role that these structures play in signaling and adhesion, and thereby in cell migration or metastasis.

At the sites of focal adhesions, clusters of transmembrane integrin receptors bind to matrix molecules and associate with a large protein complex consisting of a variety of anchor and signaling proteins and, through them, with bundles of actin filaments. Some of the known components of focal adhesions play a structural role in the maintenance and assembly of the complex, whereas others are clearly signaling molecules, essential for organizing integrin and growth factor signaling cascades. Engagement of integrin receptors by extracellular matrix components triggers signaling events including tyrosine phosphorylation cascades, pH elevation, increased synthesis of phosphatidylinositol-4,5-bisphosphate, and activation of the MAPK cascade (Petit and Thiery, 2000).

Different cellular functions require different adhesion structures, and this is reflected by the various types of cell-extracellular matrix attachments described so far: focal adhesions, focal complexes, fibrillar adhesions, and podosomes (Geiger and Bershadsky, 2001). While focal adhesions are large structures at the ends of stress fibers, focal complexes are smaller adhesion contacts at the edges of moving cells, specifically at cell protrusions such as filopodia and lamellipodia. Fibrillar adhesions are central structures that contain some of the same protein components as focal adhesions; podosomes are specialized structures found on monocytes that consist of a ring with an actin core and adhesion proteins at the periphery (Kaverina et al., 2002). Adhesion complexes originate as focal complexes, which may live briefly and turn over in just a few minutes or undergo a transition and mature to focal adhesions (Small and Kaverina, 2003). Focal complexes are thought to be an intermediate adhesive state and are required for motility; moving cells assemble focal complexes at the leading edge of the cell and disassemble them at the rear (Murphy-Ullrich, 2001; Small and Kaverina, 2003).

Over 50 proteins are reported to be involved in cellular attachment (Zamir and Geiger, 2001); however, many more proteins are likely to be present in the protein complexes responsible for this behavior. Mass spectrometry is an attractive method to investigate multiprotein complexes (Aebersold and Mann, 2003); however, one problem with protein identification from any biochemical isolation, by mass spectrometry or otherwise, is the issue of co-purifying proteins. With affinity-based isolation techniques, immunoprecipitations, and biochemically isolated subcellular structures, the preparation can be heavily contaminated with undesirable proteins originating from many different sources. We have set out to overcome these limitations using quantitative proteomics; the strategy we used was designed to reveal which proteins are interacting in an attachment-specific manner with three central players in cell adhesion.

Previously, our laboratory described a mass spectrometry-based strategy termed *s*table *i*sotope *l*abeling by *a*mino acids in *c*ell culture (SILAC) (Ong et al., 2002, 2003a, 2003b). In this method, one cell population is grown in medium containing normal amino acids, and another population in medium with deuterium-substi-

*Correspondence: mann@bmb.sdu.dk
[2]These authors contributed equally to this work.

tuted leucine or ^{13}C-labeled arginine, making their peptides distinguishable by mass spectrometry. This labeled population and a control group can then be subjected to different stimuli and combined prior to further purifications, as peptides derived from the labeled sample can be distinguished in the mass spectrometer from those peptides originating from the nonlabeled sample. During mass spectrometric analysis, the relative peak intensities between the labeled and unlabeled peptide are quantitative, providing an elegant way to evaluate the effects of a treatment on a large number of proteins in a single experiment. Heavy and light forms of peptides from proteins unaffected by the treatment will show equal intensities while those from proteins responsive to the differential condition will be more strongly represented by one form or the other. We have previously applied SILAC to identify authentic lipid raft proteins in biochemical preparations (Foster et al., 2003) and to identify signal-dependent protein interactions in recombinant protein pulldowns (Blagoev et al., 2003). Other labeling strategies have been successfully applied in a similar fashion. For example, the isotope-coded affinity tag (ICAT) method has been used to study RNA polymerase preinitiation complexes and STE12 protein complexes (Ranish et al., 2003).

In this report, SILAC was used to differentiate between proteins that have adherence-dependent and adherence-independent interactions with talin, paxillin, and vinculin isolated from floating and adherent MRC5 lung fibroblast cells. This strategy was designed to discover proteins with a functional interaction with three prominent members of focal adhesions. Identification of many proteins was expected but only those proteins that bind more strongly to one of the targets in adhered cells (revealed by the ratio of light to heavy peptides) are defined as functional, adhesion-dependent interactors. We reasoned that knowledge of the proteins that interact with these central players in cell attachment in a functional manner may reveal mechanistic details about the biology of cell attachment. Application of this strategy identified several known focal adhesion proteins as expected, along with a number of novel and unexpected proteins. A subset of these unanticipated proteins was examined by fluorescent confocal microscopy and in cell spreading assays. RACK1, reported recently to be involved in regulation of cell migration, was identified here as a protein that is bound to vinculin in an attachment-specific manner. We also demonstrate that members of two families of RNA binding proteins, Sm proteins and hnRNPs, localize specifically to a novel structure that precedes the formation of focal adhesions. This novel structure, which we have termed the spreading initiation center (SIC), is present only in early stages of cell spreading, is enclosed by an actin sheath, and also contains ribosomal RNA.

Results

Functional Analysis of the Attachment Proteome by SILAC

In order to identify proteins interacting with the central adhesion proteins talin, vinculin, and paxillin in an adhesion-dependent manner, we applied SILAC to standard immunoprecipitation procedures using lysates from attached and nonattached cells. This technique was designed to highlight attachment-dependent interactions and not merely to distinguish specific interactions from nonspecific ones. We encoded all the proteins in one of two cell populations of MRC5 human lung fibroblasts, a nontransformed cell line, by metabolically labeling with deuterium-substituted leucine, LeuD3 (Figure 1A) (Ong et al., 2002). One set of cells was lifted from the plate and maintained in suspension to allow focal adhesions to disassemble, while the other population was untreated. Equal amounts of proteins from the lysates were combined and then subjected to immunoprecipitation with monoclonal antibodies against talin, paxillin, or vinculin. Both the heavy (LeuD3) and light (Leu) forms of the targets will be precipitated in this step, in addition to protein complexes containing the target from either condition. Proteins in the immune complexes were eluted and prepared for analysis by LC-MS/MS as described in Experimental Procedures. Measured fragmentation spectra of each observed peptide were matched to the corresponding tryptic sequence in a nonredundant database of *H. sapiens* proteins to arrive at lists of identified proteins. Subsequent quantitative analysis of the mass spectra revealed attachment-dependent interacting proteins as determined by the higher peak heights of LeuD3 versus Leu peptides (Figure 1B). Peptides from proteins where the heavy and light forms precipitated equally will appear with equal intensities in the mass spectrum and thus have a ratio near 1. Among proteins expected and observed to have ratios near 1 were the respective target proteins (e.g., paxillin in the paxillin immunoprecipitate) and highly abundant cytosolic proteins (e.g., heat shock proteins, glycolytic enzymes) that bind nonspecifically to the beads. In addition, any protein that binds specifically to the target in a nonattachment-dependent manner will also have a ratio near 1.

We performed multiple, independent IPs for each of talin, vinculin, and paxillin—a total of nine different quantitative proteomics experiments. As an additional confirmation of the differentially interacting proteins, the vinculin IP was repeated in an additional experiment, labeling cells with ^{13}C6-arginine instead of LeuD3. We examined the ratios for the proteins discussed below and found differential interaction in each case, thereby increasing our confidence in the ratios obtained from the SILAC strategy. Excluding obvious contaminants such as keratins, 282 unique proteins were identified in total (see Supplemental Tables S1 and S2 at http://www.cell.com/cgi/content/full/117/5/649/DC1). Among these were many proteins already known to bind directly or indirectly to one or more of the target proteins, indicating that the immunoprecipitation strategy was working as expected. Our proteomics strategy yielded anticipated proteins along with candidates for new focal adhesion proteins, including some novel ORFs. Some previously known focal adhesion components were found in this study, including vinculin (in talin IPs), talin (in vinculin and paxillin IPs), vimentin, actin, low-density lipoprotein receptor-related protein, tubulin, CasL-interacting molecule, F actin-capping protein, ADP-ribosylation factor 1 (ARF1), and ARF GTP-exchange factor, as well as other cytoskeletal components and numerous

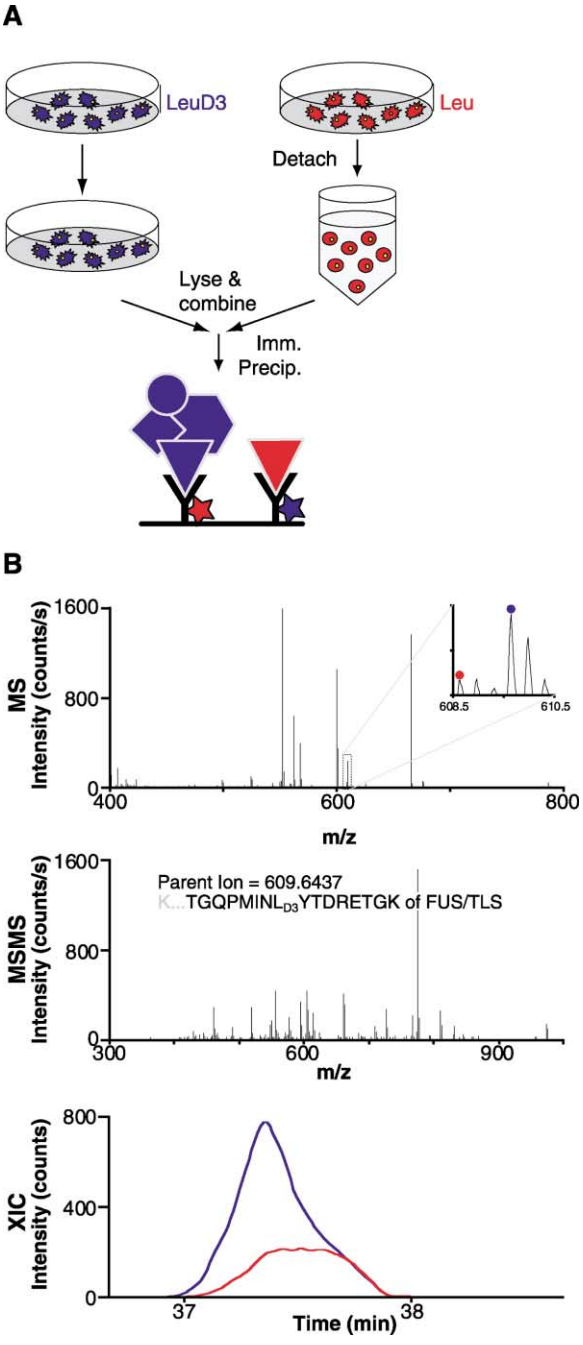

Figure 1. SILAC to Identify Attachment-Dependent Interactions

(A) Two populations of MRC5 cells are grown in leucine-deficient media, one supplemented with normal isotopic abundance leucine (Leu, red) and the other with L-leucine-*3,3,3*-D3 (LeuD3, blue). The Leu population is lifted from the substrate and incubated in suspension to allow focal adhesions to disassemble. Equal amounts of protein from the "floating" and "attached" lysates are mixed and used to IP known focal adhesion components. Proteins bound to the immunoprecipitates are eluted and prepared for LC-MS/MS analysis as described in Experimental Procedures.

(B) Peptide mixtures are resolved by nanoflow reversed phase HPLC and sprayed directly into the mass spectrometer as it continuously acquires survey spectra (MS) and information-dependent fragmentation spectra (MS/MS). Peptides are identified from fragmentation spectra using a search engine, and postacquisition processing of the survey spectra generated chromatographic profiles (extracted ion chromatograms or XICs) for the heavy and light forms of each peptide, representing the relative quantitative measure of the two.

extracellular matrix proteins (Orr et al., 2003; Turner, 2000; Zamir and Geiger, 2001) (see Supplemental Table S1 on the *Cell* website). Quantitation of all leucine-containing peptides identified revealed that only a small fraction of the 282 proteins bound differentially to one of the targets in attached versus floating cells. This fraction included many previously uncharacterized proteins such as HSPC117, KIAA0144, and KIAA1797 (see Supplemental Table S1 for differential ratios) that could potentially be novel participants in cell adhesion.

Many of the proteins identified with a ratio were not identified in all three IPs, but this would only be expected if the entire complement of each component were in a stoichiometric complex with the others. However, many of the complexes will be substoichiometric, and therefore a tertiary interaction (i.e., RACK1 interacting with paxillin via vinculin) is more difficult to detect since only a very small fraction of the tertiary interactor is present in the IP. In addition, detection of a protein in all three IPs would be expected only if vinculin, talin, and paxillin form a stoichiometric complex that engages all copies of each protein in the cell. In reality, only those proteins that have a direct attachment-dependent interaction with a given bait protein will appear in the immunoprecipitate of that bait. Those candidates can then be followed up using biochemical or microscopic methods.

RACK1 and Vinculin Localize to a Novel Structure in Actively Spreading Cells

*R*eceptor for *a*ctivated *C k*inase 1 (RACK1) is a cytosolic, WD-40 repeat protein that was originally identified based on its binding to activated protein kinase C (PKC) (Ron et al., 1994) and has recently been reported to play a role in integrin-mediated adhesion (Cox et al., 2003). It has also been shown to bind integrins, and its overexpression inhibits cell migration and increases focal adhesion number (Buensuceso et al., 2001; Liliental and Chang, 1998). In this study, RACK1 was found to bind more strongly to vinculin from adhered cells and more strongly to talin from floating cells. The opposing behaviors for vinculin and talin binding may be due to RACK1 having some measurable affinity for talin regardless of the adherence state. When participating in adhesion it may, however, be more strongly associated with vinculin. Due to the interesting pattern of observed differential ratios and the fact that it had previously been shown to be interacting with proteins found in adhesion sites, we chose to explore RACK1's involvement in cell adhesion using indirect immunofluorescence and confocal microscopy. In fully attached cells (seeded on coverslips $\geq$24 hr prior to experiment), focal adhesion components have a very distinct morphology typified by the vinculin staining in Figure 2A (center panel), namely a light, diffuse cytosolic staining with strongly stained, elongated structures on the ventral plasma membrane. Conversely, RACK1 was largely localized to nuclei and cytosolic punctae (Figure 2A), showing very little overlap with vinculin in focal adhesions.

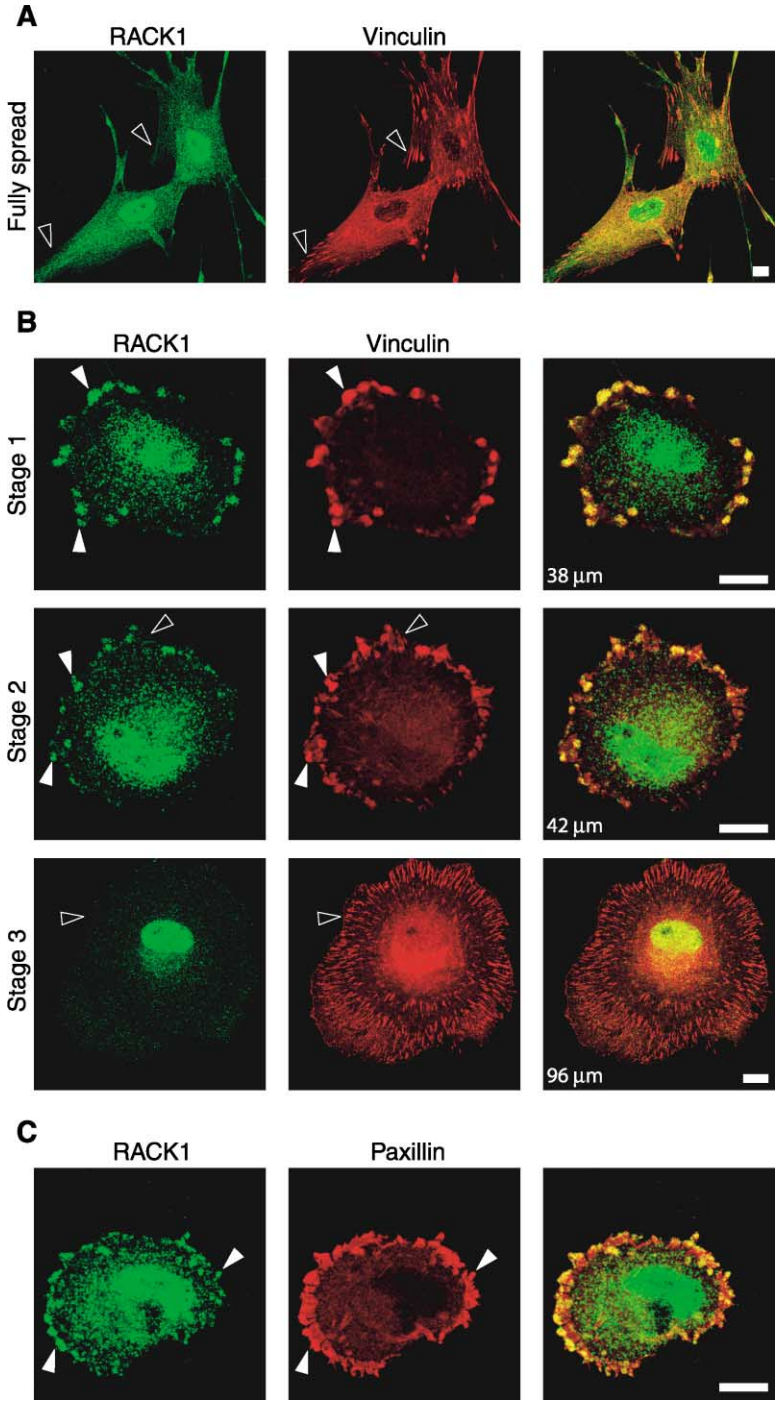

Figure 2. RACK1 Localizes to Large Circular Patches Called Spreading Initiation Centers (SICs) in Early Stages of Cell Spreading, but Does Not Localize to Mature Focal Adhesions

(A) MRC5 cells stained with RACK1 and vinculin antibodies. Open arrowheads indicate focal adhesions where no overlap exists between RACK1 and vinculin staining.

(B) Stage 1 (top panels), stage 2 (middle panels), stage 3 (lower panels) MRC5 cells stained with RACK1 and vinculin antibodies. Diameters of spreading cells in different stages are shown. Filled arrowheads indicate areas of overlap between RACK1 and vinculin staining; open arrowheads indicate no overlap in focal adhesions.

(C) MRC5 cell in the second stage of spreading stained with RACK1 and paxillin antibodies. Arrowheads indicate areas of overlap between RACK1 and paxillin staining. Scale bars represent 10 μm.

It seemed unlikely that the presence of RACK1 in the immunoprecipitates could be attributable to the weak overlap in cytosolic staining observed between vinculin and RACK1 since this would provide no obvious explanation for the attachment dependence of the interactions. A recent report (Cox et al., 2003) suggested that RACK1 colocalizes at the leading edge of migrating cells with a subset of nascent focal adhesions that contain paxillin but not vinculin. Therefore, we explored the morphological changes that focal adhesion components undergo in the process of cell spreading after initial attachment and the possible role of RACK1 in these steps. To achieve this, MRC5 cells were nonenzymatically lifted from their substrate, maintained in suspension for 1 hr to allow focal adhesion complexes to dissociate, and then replated on coverglass to attach and begin spreading prior to processing for indirect immunofluorescence (see Experimental Procedures). Fluorescent confocal imaging of these cells revealed at least three distinct stages of spreading that cells undergo after initial attachment. In stage 1, when the cells have spread to a diameter of ~35 μm, vinculin is not

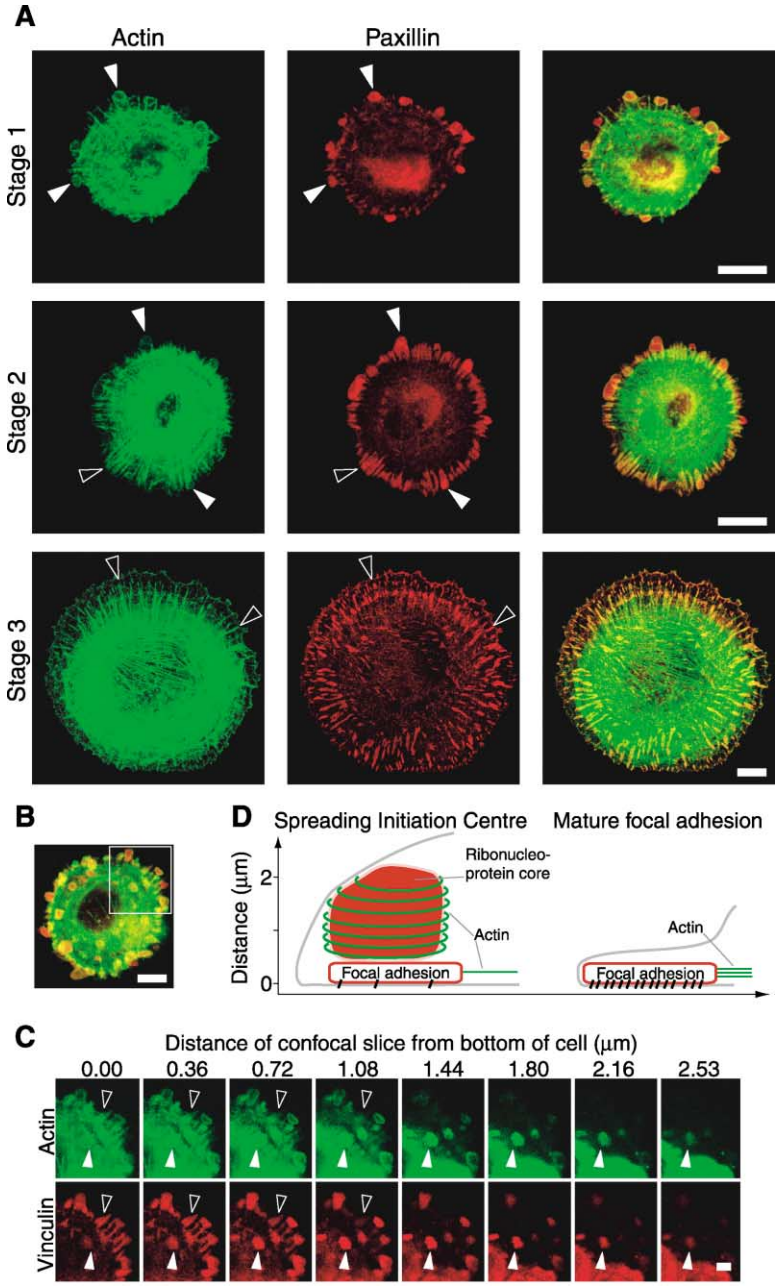

Figure 3. Actin Seems to Form a Sheath around SICs

MRC5 cells were maintained in suspension for 40 min to allow focal adhesion disassembly prior to replating on coverglass. (A) Stage 1 (top panels), stage 2 (middle panels), and stage 3 (bottom panels) cells with filamentous actin visualized using Alexa488-phalloidin and stained for paxillin. Filled arrowheads indicate SICs surrounded by actin rings. Open arrowheads indicate focal adhesions with anchored actin fibers. Scale bars represent 10 μm. (B) An MRC5 cell stained with Alexa488-phalloidin and vinculin antibody. Scale bar represents 10 μm. The outlined area is magnified and shown in the Z dimension in (C): confocal slices were imaged through the cell and distances between the bottom slice and the center of each higher slice are given. Scale bar represents 2 μm. (D) A schematic showing the architecture of a SIC and a focal adhesion.

seen in focal adhesions per se but rather in much larger, circular patches approximately 2 μm across (Figure 2B, top center panel). As cells become slightly more spread, these patches become less abundant and focal adhesion complexes start to appear beneath them (stage 2, Figure 2B, middle center panel). At later stages of spreading, the circular patches disappear altogether and vinculin is only seen in classical focal adhesions (stage 3, Figure 2B, bottom center panel). These stages are defined by their staining patterns as well as the increasing diameter of the cells from stages 1 to 3, and we interpret the increasing cellular diameters from stages 1 through to 3 to mean that cells progress through these stages in numerical order. We have termed the distinctive patches "spreading initiation centers" (SICs). Double-labeling of RACK1 in the same cells revealed that the RACK1 punctae described above are more concentrated in SICs, colocalizing extensively with vinculin in these patches but not at all in mature focal adhesions (Figure 2B, left panels). We stained spreading MRC5 cells for RACK1 and paxillin (Figure 2C) and found that paxillin in SICs colocalized with RACK1 to a similar extent as vinculin.

Actin Forms a Sheath around Spreading Initiation Centers

One of the main functions of focal adhesions is to act as anchors for the actin cytoskeleton: actin stress fibers normally terminate at focal adhesions. Given that spreading initiation centers precede mature focal adhe-

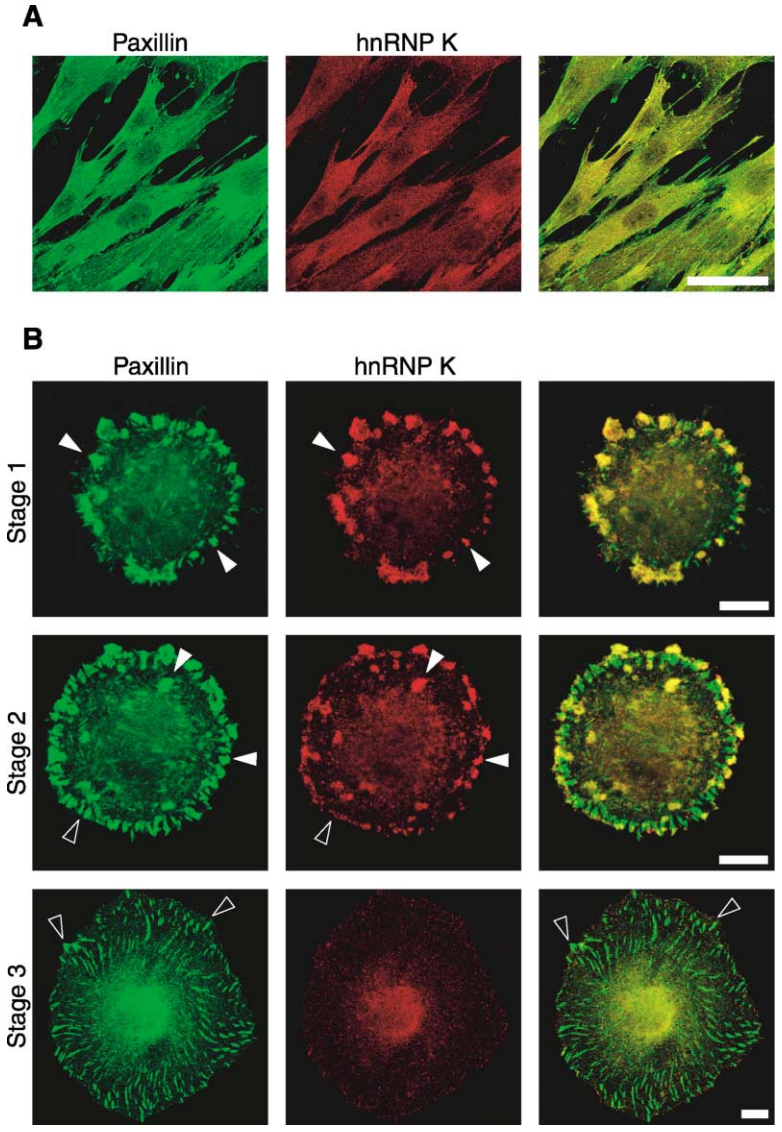

Figure 4. RNA Binding Protein hnRNP K Localizes to SICs but Not to Focal Adhesions

Filled arrowheads indicate areas of overlapping staining of paxillin and hnRNP K in SICs. Open arrowheads indicate focal adhesion complexes where no overlap exists. (A) MRC5 cells stained with hnRNP K and paxillin antibodies. Scale bar represents 50 μm. (B) Stage 1 (top row), stage 2 (middle row), and stage 3 (bottom row) spreading cells stained with hnRNP K and paxillin antibodies. Scale bars represent 10 μm.

sions, we then characterized the involvement of actin in SICs. Paxillin staining patterns were very similar to those seen for vinculin in all three stages of spreading described above (compare center panels of Figures 2B and 3A). However, actin was excluded from the SICs themselves, instead forming a ring around them. In stage 1 cells, the actin cortex and stress fibers have started to form and the rings around the SIC are most prominent (Figure 3A, top panels). As cells spread further, the stress fibers, anchored to mature focal adhesions, become more apparent and although the number of SICs generally decrease, they are still surrounded by actin rings (Figure 3A, middle panels). In later stages of spreading, the SICs and their associated actin rings disappear and each mature focal adhesion has become an anchor point for an actin stress fiber (Figure 3A, bottom panels). Three-dimensional imaging of the actin rings revealed that they appear to be domes or sheaths of actin surrounding the entire SIC (Figures 3B and 3C). Classical focal adhesions are found almost entirely within 1 μm of the ventral plasma membrane. Moving vertically through the cell, the focal adhesion staining decreases while the SIC staining begins and extends more than 2 μm above the bottom of the cell. Based on these observations, a model of a SIC in relation to stress fibers and focal adhesions is illustrated in Figure 3D. Our observations also indicate that SICs are distinct from podosomes, rosettes, and invadopodia, all of which are known adhesion-related structures.

Some of the other classical markers for focal adhesions include focal adhesion kinase (FAK), talin, and extensive tyrosine phosphorylation. SICs also contain talin (Supplemental Figure S1) and FAK (Supplemental Figure S2A), and while there is some detectable phosphotyrosine, it is not as strong as that seen in mature focal adhesions (Supplemental Figure S2B).

RNA Binding Proteins Localize to SICs

Several unexpected proteins were observed differentially bound to the talin, vinculin, and paxillin immunoprecipitates. We were especially intrigued by the well-represented class of RNA binding proteins; many of

these, including FUS/TLS, hnRNP I, hnRNP K, hnRNP Q2, JKTB, and Sam68, had ratios indicating preferential binding to one of the target proteins in attached cells (see Supplemental Table S1). The unexpected presence of RNA binding proteins and the specificity of their association supported by their differential ratios by quantitative proteomics led us to investigate the role of this class of proteins in adhesion and spreading. In fully spread MRC5 cells, hnRNP K shows a punctate cytosolic distribution (Figure 4A), as has been reported (Habelhah et al., 2001) but is not present in focal adhesions stained with antibodies against paxillin. However, in stage 1 and stage 2 spreading cells, cytosolic hnRNP K concentrates almost exclusively in SICs with very little staining seen outside vinculin-delineated SICs. Furthermore, hnRNP K behaved similarly to RACK1, as it was not visible in mature focal adhesions in later stages of spreading (Figure 4B). FUS/TLS and hnRNP E1 also behaved in this way, localizing to SICs in early spreading cells and dispersing in later stages (see Figure 6 and Supplemental Figure S2).

The Sm proteins were another well-represented family of RNA binding proteins observed to bind differentially to the target proteins in attached versus floating cells. Sm proteins form a heteromeric ring structure that complexes with a stable U RNA to form an snRNP (Will and Luhrmann, 2001). Several of these snRNP particles associate with the spliceosome in the nucleus, but the Sm proteins themselves have only a structural role in this complex and have no enzymatic RNA-processing function. Again, indirect immunofluorescence was used to test whether Sm proteins colocalize with focal adhesion components. Since only antibodies raised in mouse were available against both Sm proteins and focal adhesion components, cells were double-labeled with antibodies against Sm B, Sm D, or the snRNP U1 complex and phalloidin to detect actin; in this case, SICs could be detected by the existence of the actin rings described above. In fully spread MRC5 cells, actin is seen in stress fibers and membrane ruffles and there is no detectable Sm staining outside of the nucleus (Figure 5A). However, in actively spreading cells, a portion of Sm B and D can be detected in the cytoplasm. Interestingly, this nonnuclear Sm protein population localizes specifically to SICs marked by actin rings (Figure 5B). As additional biochemical evidence, Sm B and Sm D were also detected in the immunoprecipitates by Western blotting (data not shown). However, antibodies against the entire snRNP U1 complex did not stain SICs under similar conditions (Figure 5B), indicating that at least this snRNP particle is not found in SICs. The transient presence of Sm B and D in the cytosol is not simply a bulk movement of nuclear proteins to SICs since histone H3 was undetectable in SICs in stage 1 or stage 2 cells (Supplemental Figure S1).

SICs Occur in Other Cell Types and on Defined Substrates

We wondered if SICs were a feature specific to MRC5 cells, so we tested six other cell types, including NIH 3T3, HEK 293, human umbilical vein endothelial cells, HeLa, primary mouse embryo fibroblasts (MEFs), and WS1, a human skin fibroblast cell line. WS1 and MEFs form SIC-like structures surrounded by actin, containing paxillin, vinculin, hnRNP E1, and hnRNP K after 50 min of spreading (Figure 6A). Interestingly, nothing similar was observed in any of the transformed or nonfibroblastic cell types. NIH3T3 cells are shown in the lower panel of Figure 6A; it is worth noting that these cells form focal adhesions at a much earlier stage of spreading than do MRC5 cells. We also tested whether the defined substrates could support SIC formation by replating cells on coverslips coated with fibronectin, gelatin, or poly-L lysine; SICs form on the physiological substrates fibronectin and gelatin, but not on the nonphysiological substrate poly-L lysine (Figure 6B).

In addition, we tested whether migrating cells form SICs by performing wound-healing assays and do not detect SIC formation in this situation (data not shown); however, we did not expect to find SICs under these conditions, as cell migration in many respects is distinct from cell spreading.

SICs Contain Ribonucleic Acids

Given that RNA binding proteins are present in SICs, we next investigated whether RNA itself is present in these complexes using the nucleic acid binding fluorophore SYTOX Orange. Stage 1 (Figure 7A, top panels) and stage 2 (results not shown) cells showed significant colocalization between paxillin and SYTOX, indicating that nucleic acid is also present in SICs. Treatment of the cells with RNase I (Figure 7A) or RNase A (results not shown) eliminated all cytoplasmic and SIC-localized nucleic acid staining, indicating that the staining in SICs is specific and is indeed due to RNA and not DNA. In parallel with the behavior of the RNA binding proteins discussed above, no RNA was observed in mature focal adhesions present in later stages of spreading (Figure 7B).

Mammalian cells contain many different types of RNA, so it was not immediately obvious what kind(s) caused the staining seen in Figure 7A. The mRNA coding for actin has been previously observed in lamellipodia (Kislauskis et al., 1997; Lawrence and Singer, 1986), so mRNAs for actin or other proteins involved in adhesion could be present in SICs to allow rapid production of such proteins at the sites where they are needed. In addition, if mRNA were being translated in SICs, then ribosomes and ribosomal RNA should also be present and, in fact, several ribosomal proteins were identified in the immunoprecipitates described above. We synthesized fluorescently labeled oligonucleotides complementary to actin and FAK mRNA as well as to the 18S ribosomal RNA and used them to ask, via a fluorescent in situ hybridization assay, if any of these molecules were present in SICs. Note that it is not possible to use antibodies against other SIC proteins to double-label the cells in this assay because of the harsh hybridization conditions required. Nonetheless, the rRNA probes displayed a reticular staining pattern, consistent with the localization of ribosomes in the endoplasmic reticulum, in addition to strongly staining SICs in early spreading cells (Figure 7C). Actin and FAK mRNA probes only labeled isolated punctae in the nucleus (data not shown), with no detectable staining in SICs.

The Sm proteins identified here can participate in very well-defined ribonucleoprotein particles with some of

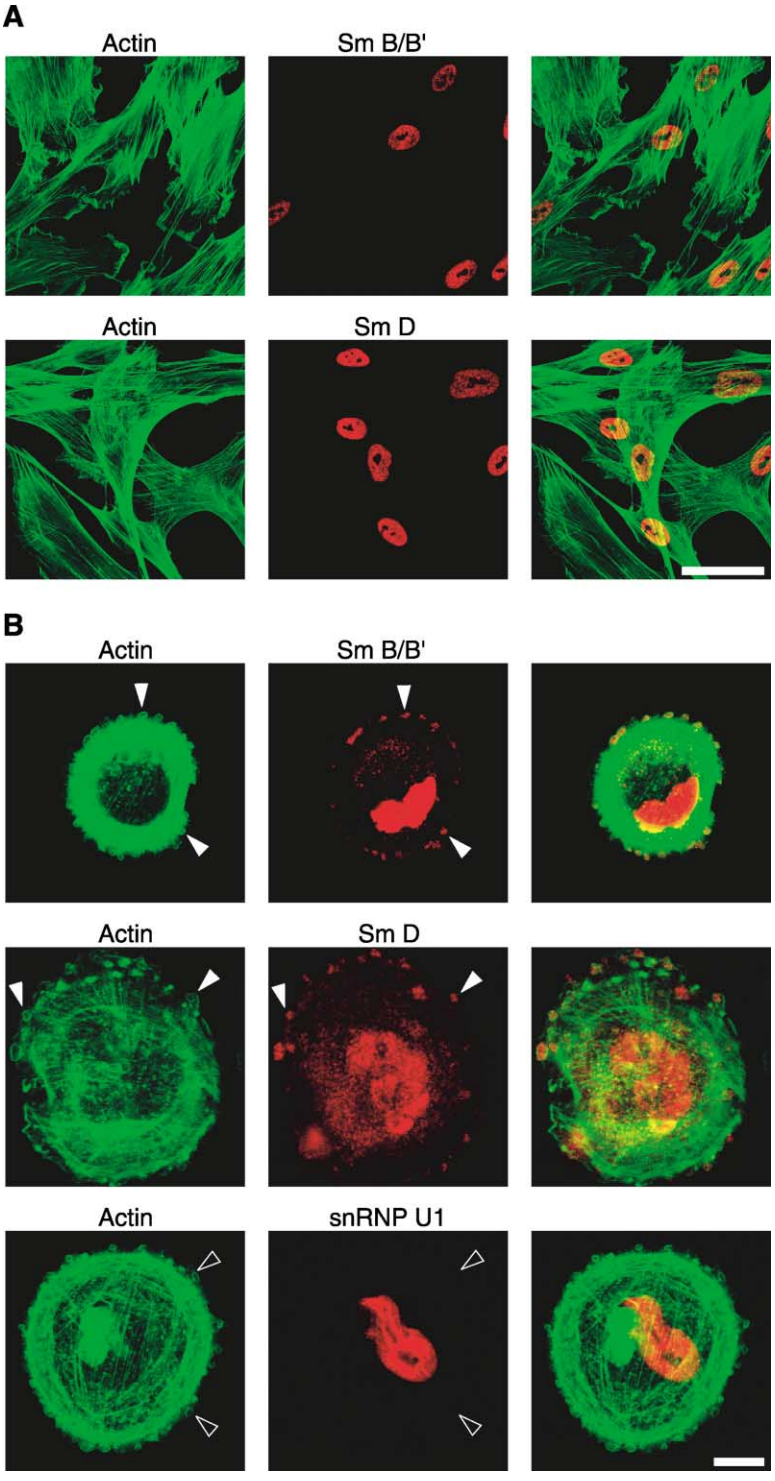

Figure 5. Sm Proteins B and D Localize to SICs

(A) MRC5 cells plated 24 hr prior to staining with Alexa488-phalloidin and anti-Sm B (top panels) or anti-Sm D (bottom panels). Scale bar represents 50 μm. (B) MRC5 cells were maintained in suspension for 40 min prior to replating on coverglass. Shown are cells representative of stages 1 or 2 stained with Alexa488-phalloidin and antibodies against Sm B (top panels), Sm D (middle panels), or the snRNP U1 complex (bottom panels). Filled arrowheads indicate Sm B or D staining in SICs surrounded by actin rings. Open arrowheads indicate SICs lacking snRNP U1 staining. Scale bar represents 10 μm.

the snRNAs (Will and Luhrmann, 2001). Using a sensitive reverse transcriptase primer extension assay, we were unable to find evidence for any of the spliceosomal snRNAs in immunoprecipitates of vinculin or hnRNP K from either floating or attached cells (Figure 7D). Additionally, antibodies against the 2,2,7-trimethylguanosine (TMG) cap of U snRNAs stain in the nucleus very clearly but do not detect any TMG in SICs (Figure 7E).

FUS/TLS and hnRNPs Function in Cell Spreading

After demonstrating that RNA binding proteins are present in SICs, we next assessed whether they play a role in cell spreading. If the RNA binding proteins do have a functional role, then interfering with them should affect this process. To functionally test this hypothesis, antibodies against hnRNP K, hnRNP E, and FUS/TLS were introduced into suspended MRC5 cells and the cells

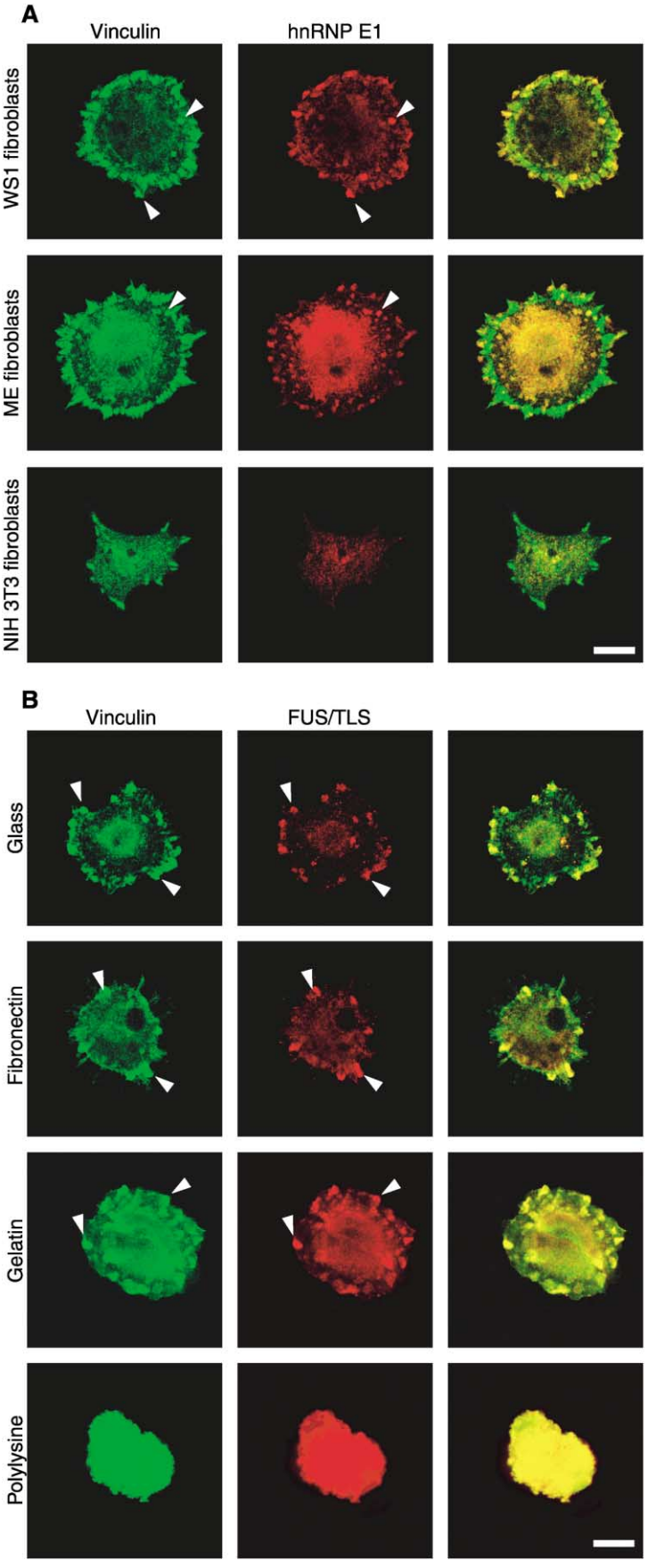

Figure 6. SICs Form in Other Cell Types and on Various Substrates

Cells were maintained in suspension to allow focal adhesion disassembly prior to being replated on coverslips for 50 min. Scale bars represent 10 μm. (A) SICs are not exclusive to MRC5 cells. WS1, MEFs, and NIH3T3 cells were stained with antibodies against vinculin and hnRNP E1. (B) SICs form on various substrates. MRC5 cells were replated onto coverslips coated with fibronectin, gelatin, or poly-L lysine or were plated onto uncoated glass coverslips and stained with antibodies against vinculin and FUS/TLS. Filled arrowheads indicate areas of overlapping staining in SICs.

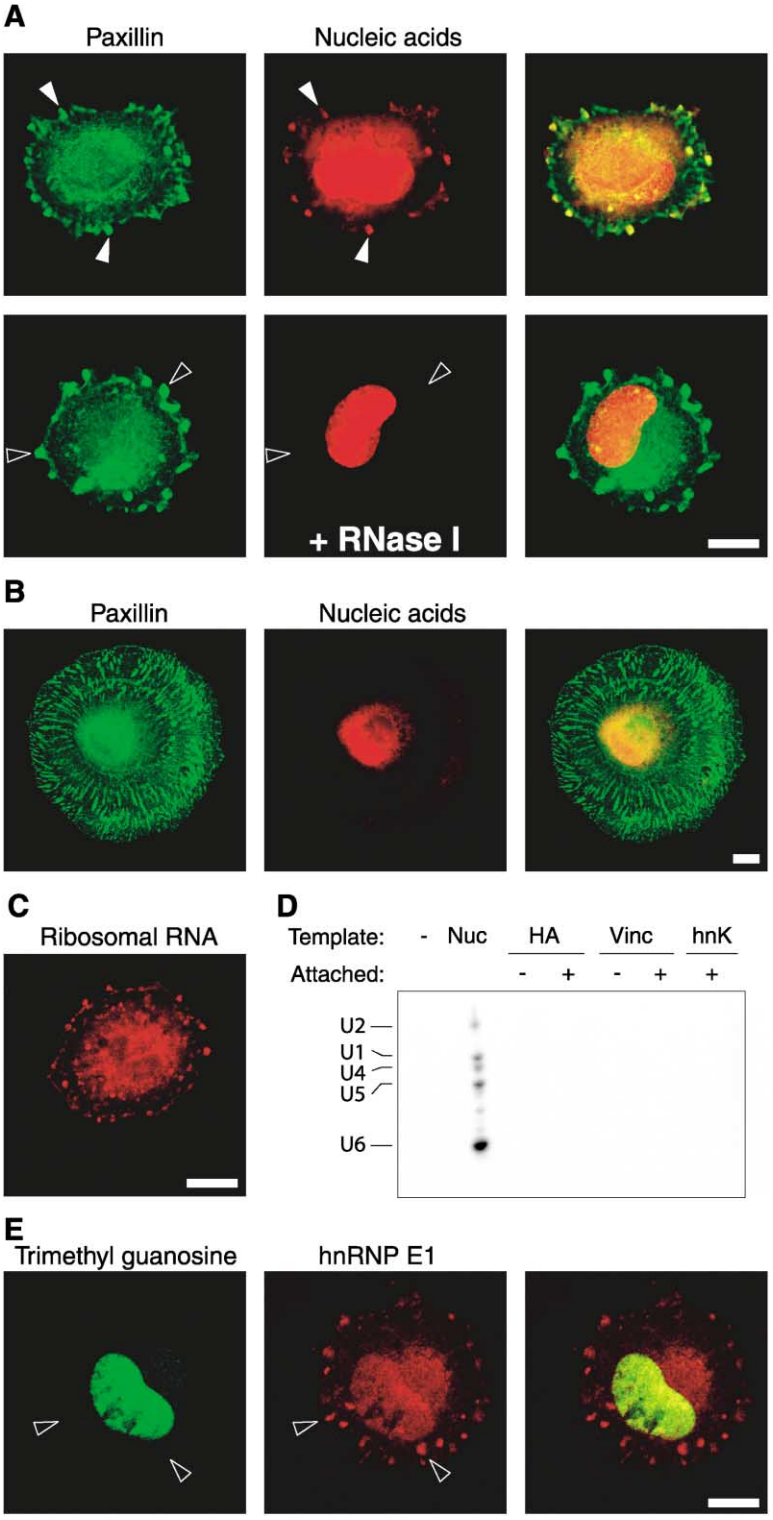

Figure 7. RNA Localizes to SICs in Early Stages of Cell Spreading

(A) Stage 1 spreading MRC5 cells stained with paxillin antibody and SYTOX Orange. Prior to staining with SYTOX, the cells were treated with buffer alone (top panels) or 5 U/ml RNase I for 20 min (bottom panels). Filled arrowheads indicate areas of overlapping staining of paxillin and nucleic acid in SICs. Open arrowheads indicate SICs with no overlap due to RNase treatment.

(B) Stage 3 spreading MRC5 cells stained with paxillin antibody and SYTOX Orange.

(C) Fluorescent in situ hybridization of 18S ribosomal RNA probes in spreading MRC5 cells.

(D) Vinculin (Vinc), hnRNP K (hnK), and hemagglutinin (HA) IPs were performed on lysates from floating (−) and attached (+) cells. Nuclear extract (Nuc) as well as RNA isolated from the IPs or beads alone (−) was used in an RNA extension assay as described in Experimental Procedures. Resulting ^{32}P-labeled products were resolved by urea-formaldehyde gel electrophoresis and detected by exposure to X-ray film for 1.5 hr. Longer exposures did not reveal any more bands in any of the lanes. The positions of U1, U2, U4, U5, and U6 snRNAs are indicated.

(E) Stage 1/2 spreading MRC5 cells stained with 2,2,7-trimethylguanosine and hnRNP E1 antibodies. All scale bars represent 10 μm.

were then allowed to attach for 80 min. Mouse IgG and vinculin antibodies were used as negative controls and FAK antibody was used as a positive control. The cells were fixed, stained for talin or vinculin, and a qualitative assessment of the radius of the staining pattern from this process was used as a measure of cell spreading (Figure 8A) as described in Experimental Procedures. Approximately 24% of cells electroporated with nonimmune mouse IgG had started to spread within 80 min of replating. Cells electroporated with vinculin antibodies were significantly retarded in their ability to spread while cells that received FAK antibodies spread farther (Figure

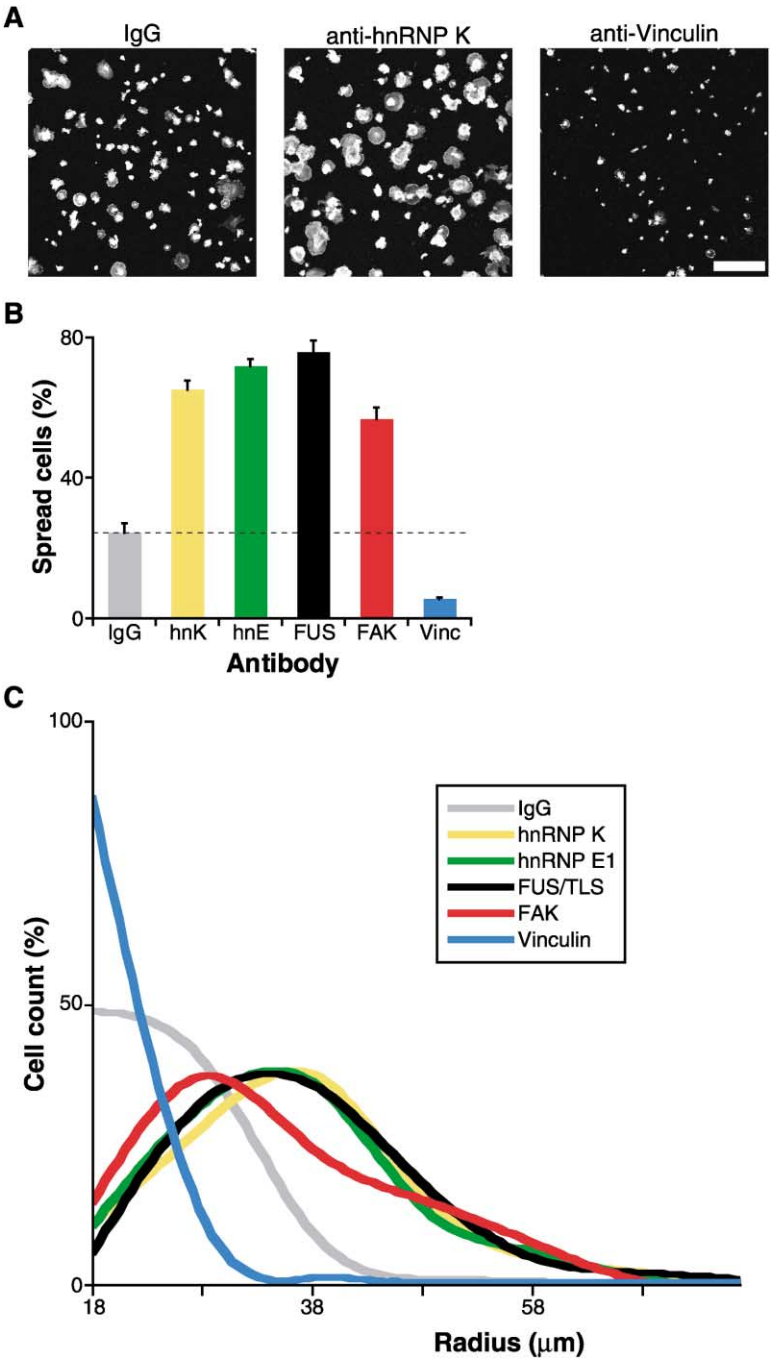

Figure 8. Perturbing RNA Binding Proteins Affects Cell Spreading

MRC5 cells were maintained in suspension to allow focal adhesion disassembly prior to electroporation in the presence of antibodies as described in Experimental Procedures. After replating on coverglass, the cells were fixed and stained with talin or vinculin antibodies. (A) Representative fields from cells electroporated with preimmune IgG (left), hnRNP K (middle), or vinculin antibodies (right). Scale bar represents 100 μm. (B) Average (+ SE) number of spreading cells after electroporation of indicated antibodies (IgG, preimmune IgG; hnK, hnRNP K; hnE1, hnRNP E1; FUS, FUS/TLS; FAK, focal adhesion kinase; Vinc, vinculin). Dotted line indicates the level of the control. (C) Distribution of measured radii of antibody-electroporated cells counted as "spreading" in (B). Cells with a radius less than twice that of the nucleus (approx. 18 μm) were considered "not spreading" (see Experimental Procedures).

8B). Interestingly, antibodies against FUS/TLS, hnRNP K, and hnRNP E1 all had an even greater stimulatory effect on spreading than did FAK (Figure 8B). Parallel quantitative measurements of the radii of these cells revealed that those reagents that increased the number of cells spreading also increased the average radii of those cells (Figure 8C).

Discussion

Cell attachment has been studied intensively for 30 years, resulting in a great number of proteins being described as direct residents of focal adhesions or as indirect components binding to a more central player (Turner, 2000; Zamir and Geiger, 2001).The particular strategy chosen here was not designed to give a comprehensive overview but instead to reveal attachment-specific interaction partners of key focal adhesion components. The improving sensitivity of mass spectrometers combined with available genome data and improved search algorithms provide proteomic studies with ever-growing lists of identified proteins. However, these are also increasingly plagued with specificity issues. To address these, we employed a functional

screen that utilized the power of quantitative proteomics to specifically discover attachment-dependent interactions. The functional information indicated that, surprisingly, numerous RNA binding proteins are potentially involved in cell attachment and provided the impetus to study these surprising interactions. The emphasis of this study was not a proteomic investigation of focal adhesions and as such we only followed up on a small number of these differentially binding proteins here. This leaves many intriguing candidates that will require confirming experiments to establish their involvement, if any, in cell adhesion (see Supplemental Tables for the complete list of proteins and their attachment ratios).

In this study, we identified a novel structure, which we have termed the spreading initiation center (SIC), that appears during the early stages of cell spreading. The protein composition of SICs and focal adhesions seems to be very similar with respect to classical focal adhesion components and related, known structures but dramatically different with respect to RNA, RACK1, and the RNA binding proteins identified in the proteomics experiments described here. FUS/TLS, hnRNP K and E1, and Sm B and D are all clearly in SICs but we have found no evidence of their presence in mature focal adhesions. SICs are also distinct from focal adhesions/focal complexes on a structural level: (1) rather than containing actin themselves they appear to be surrounded by an actin sheath, (2) they are found much further from the ventral membrane than are focal adhesions (Figure 3), (3) they are round rather than sharply defined, elongated structures like focal adhesions, and (4) SICs contain RNA, making them ribonucleoprotein complexes, while focal adhesions do not. Since ribosomal RNA is present, it seems possible that there is also translation of mRNA into protein, perhaps to fuel the production of focal adhesions. This hypothesis correlates with our observation that SICs always seem to form directly above classical focal adhesions where they could be local protein factories producing the required components of focal adhesions. However, our data indicate that actin and FAK mRNA are not among the messages being translated, so, while beyond the scope of this study, it will be interesting to determine which messages are present.

Of the many RNA binding proteins identified here, only polyadenylate binding protein 1 had been previously reported to interact with a known focal adhesion protein (Woods et al., 2002), so the hnRNPs, Sm proteins, and other similar proteins bound to talin, paxillin, or vinculin required further confirmation. We have established several lines of evidence that all indicate that these proteins are involved in adhesion and are authentic interacting partners: (1) they bound differentially to the target proteins, indicating that their interaction is specific and dependent on the adherence state of the cell; (2) each protein was reproducibly identified in multiple experiments with each immunoprecipitated protein; (3) an arginine-based SILAC experiment also identifies these proteins; (4) indirect immunofluorescence placed all of the tested proteins in SICs; and (5) perturbing the proteins affected cell spreading.

The observations that functional interference with hnRNPs and FUS/TLS leads to increases in cell radii indicate that the effect of the interference may be one of rate control rather than as a switch that triggers the cells to start spreading. In any case, the fact that these reagents have an effect on cell spreading strongly suggests that these proteins play a functional role in this process.

The Sm proteins identified here are also found in the spliceosome but they do not have an enzymatic role in that complex. An snRNP particle consists of the Sm protein core where the Sm proteins form a seven-membered ring structure around the snRNA (Kambach et al., 1999). Sm proteins have, therefore, merely a structural role in that they bind the small, stable snRNAs; since the snRNAs and snRNP U1 do not appear to be present, it is unlikely that any splicing is occurring in SICs. The hnRNP family is comprised of $\sim$20 proteins that were originally identified as binding mRNA in the cell nucleus; they possess various RNA binding domains that directly interact with RNA, often in a sequence-specific manner (Krecic and Swanson, 1999). This diverse protein family is likely to have different and perhaps unique functions, helping to package pre-mRNA into functional complexes; hnRNP K and hnRNP E1/E2 have proposed roles in translational silencing (Krecic and Swanson, 1999; Ostareck-Lederer et al., 2002). Therefore, it is unlikely that the RNA binding proteins identified here are participating in an RNA-processing event; rather, it is likely that they are bound to RNA in a protective or stabilizing role.

In the past few years, RNA has been implicated in many novel functions apart from its classical roles as tRNA, mRNA, and rRNA. Recently intense interest has focused on microRNAs and small interfering RNAs (siRNAs) because of their ability to silence genes at both the transcriptional and translational levels (Pickford and Cogoni, 2003). Ribonucleoproteins also have roles that are not related to the transcription/translation process. Protein folding is partially assisted by the signal recognition particle while multidrug resistance is thought to be mediated by the vault complex; both systems are large and mostly cytosolic ribonucleoprotein complexes (Meli et al., 2001). These and various other functions of RNA fall into broad categories: gene regulation/silencing (miRNA, siRNA), ribosome maturation (snoRNA), and RNA processing (snRNA, snoRNA), replication (telomerase RNA), translation (rRNA, tRNA), transport (vRNA), and folding (signal recognition particle) (Meli et al., 2001). The data in this study support an additional category of RNA action: involvement in cell adhesion.

In conclusion, we have described a novel structure that is distinct from focal adhesions and is likely to be a precursor to focal adhesions. These structures, SICs, only appear in primary or non-tumor-derived cells and only during very early stages of spreading. Neoplastic cells have lost their anchorage dependence and are thus less dependent on the formation of focal adhesion structures for cell survival, correlating with the absence of SICs in these cells. Furthermore, using a combination of functional proteomics and immunofluorescence microscopy, we have demonstrated that two families of RNA binding proteins, along with ribosomal RNA itself, localize specifically to SICs and that at least three of these proteins, hnRNP K, hnRNP E1, and FUS/TLS, are functionally involved in controlling the rate of cell spreading.

Experimental Procedures

Materials

The following antibodies were used in this study: mouse anti-paxillin (used at 1:200 for immunofluorescence) and mouse anti-focal adhesion kinase (1:100, BD Biosciences), mouse anti-trimethylguanosine (1:100, Oncogene), mouse anti-talin (1:40) and mouse anti-vinculin (1:100, Sigma), goat anti-hnRNP K, anti-hnRNP E1, and anti-FUS/TLS (1:100, Santa Cruz Biotechnologies), Alexa488-conjugated chicken anti-mouse and -goat (1:250, Molecular Probes), Cy3-conjugated anti-goat, -rabbit, and -mouse (1:250, Jackson ImmunoLabs). Mouse anti-Sm B/B′, Sm D, and snRNP U1 were kind gifts from Dr. Ger Pruijn (Katholieke Universiteit, Nijmegen, Netherlands). Specificity of anti-hnRNP K was confirmed using the immunizing peptide to block staining (see Supplemental Figure S1B). Specificity of anti-Sm B/B′ and Sm D antibodies was demonstrated previously (Pruijn et al., 1997). SYTOX orange and Alexa488-phalloidin were purchased from Molecular Probes; mouse IgG were obtained from Sigma; and RNases A and I were purchased from Roche.

SILAC Labeling and Cell Culture

Two populations of MRC5 cells (ATCC) were grown in leucine-deficient DMEM, supplemented with 10% (v/v) dialyzed fetal bovine serum (FBS), 1 mM sodium pyruvate, 100 U/ml of penicillin and streptomycin, 2 mM L-glutamine, and 10 ml/l MEM nonessential amino acids (Invitrogen). One population was supplemented with L-leucine (Leu, Sigma) and the other with 99% isotopic abundance L-leucine-*3,3,3*-D3 (LeuD3, Aldrich) (Ong et al., 2002, 2003a). In a separate experiment, cells were labeled with ^{13}C6-labeled arginine (Cambridge Isotope Labs) (Ong et al., 2003b). Each population was grown for at least three passages encompassing a minimum of seven population doublings.

Immunoprecipitations

Vinculin, talin, or paxillin antibodies were dialyzed against PBS and covalently attached to NHS-activated sepharose (Amersham). Five 14 cm plates of LeuD3 cells were serum-starved for 18 hr, washed with PBS, placed on ice, and lysed in lysis buffer (20 mM Tris-HCl, pH 7.5; 50 mM NaCl; 1% NP40; 3 mM $MgCl_2$; 1 mM $CaCl_2$; 1 mM Na_3VO_4; 10 mM NaF; 50 mM $Na_4P_2O_7$) plus protease inhibitors (EDTA-free Complete Tablets, Roche). Five 14 cm plates of Leu cells were serum-starved for 18 hr and the cells lifted using Cell Dissociation Buffer (Invitrogen). The cells were then diluted into 35 ml of serum-free medium, incubated with gentle agitation for 60 min at 37°C, pelleted, and lysed. Equal amounts of protein from each clarified lysate were mixed and used for immunoprecipitations; IPs were precleared using goat anti-mouse IgG-agarose (Sigma), then incubated with immobilized antibodies and rocked at 4°C for 2 hr, washed four times with 1 ml of lysis buffer and protein complexes eluted in 6 M urea/2 M thiourea (in 10 mM Tris-HCl, pH 8.0)

LC/MS/MS, Database Searching, and Quantitation

Peptide digests were prepared, analyzed, and verified as described previously (Foster et al., 2003). Proteins were quantified in all cases unless no leucine-containing peptides were observed or no unambiguous peptide signal could be extracted. Quantifiable proteins whose peptides were only detected in the light form (LeuD3/Leu $<$ 0.1) were considered contaminants as they likely arose from external sources and are listed in Supplemental Table S2 online.

Immunocytochemistry and Fluorescent Microscopy

We could not observe any structures in floating cells and so focused on attached cells. For Figure 5B, coverslips were coated with 100 μg/ml fibronectin (Sigma) for 1 hr at r.t.; 2% gelatin (Sigma) for 2 hr at 4°C; or with 0.01% poly-L lysine (Sigma) for 2 hr at r.t. All coverslips were rinsed with PBS prior to addition of cells. Cells were fixed in 4% formaldehyde in PBS (all PBS solutions contained 1.04 mM $MgCl_2$ and 0.9 mM $CaCl_2$) for 10 min on ice. Excess formaldehyde was reacted with 50 mM NH_4Cl in PBS for 5 min, cells were permeabilized with 0.1% Triton X-100 for 20 min, and nonspecific IgG binding sites were blocked for 20 min with 3% BSA/3% horse serum in PBS. Antibody incubations were 1 hr each and coverslips were washed 4× with PBS after each. In situ hybridizations using oligo probes (see Supplemental Data for oligo sequences) were performed exactly as described (Latham et al., 2001; Shestakova et al., 2001). Coverslips were mounted on glass slides and imaged using a Zeiss Axiovert 200M laser scanning confocal microscope 510. Pinhole settings were adjusted to give a confocal depth of 0.5 to 0.7 μm.

Cell Spreading Assay

Cells were lifted using Cell Dissociation Buffer, pelleted, resuspended in serum-free MEM, and incubated with gentle agitation for 40 min at 37°C. The cells were pelleted, resuspended in PBS containing antibodies (20 μg/ml) against specific proteins as well as FITC-BSA (100 μg/ml), and then electroporated (0.95 nF/250 V) using a Gene Pulser II (BioRad). Cells were then washed once with PBS and placed in MEM/10% FBS on glass coverslips for 80 min before preparation for immunocytochemistry. After staining for either vinculin or talin, the samples were imaged using a 10× objective. Electroporation efficiency based on FITC-BSA was estimated to be at least 99%. Multiple fields were imaged from each condition and cells were scored blindly as either "not spreading" or as "spreading" if the outer diameter of vinculin or talin staining was greater than twice the diameter (measured using ImageJ [NIH]) of an attached, unspread cell (approximately 18 μm) (Wade et al., 2002). Approximately 500 cells were counted and measured for each condition.

RNA Assay

IPs were performed as described above from floating or attached cells. Ten microliters of nuclear extract was used as a positive control. The samples were treated with proteinase K for 20 min at 65°C and the RNA bound to RNA Tack Resin. Samples were washed 2× with 75% ethanol, dried for 5 min and the RNA diluted in Superscript buffer containing primers for U1, U2, U4, U5, and U6 snRNA (3 pmol). The samples were heated to 50°C and then dNTPs, ^{32}P-dCTP, and Superscript II reverse transcriptase (Invitrogen) were added. Samples were incubated at 42°C for 50 min and then the products were precipitated, washed, and separated on a urea-formaldehyde acrylamide gel that was then dried and exposed to X-ray film.

Acknowledgments

C.L.d.H. was supported by a Canadian Institutes of Health Research Postdoctoral Fellowship and L.J.F. by an EMBO Long-term Fellowship. CEBI is supported by the Danish National Research Foundation and the Danish Biotechnology Instrument Center. We are grateful to Dr. Angus Lamond for helpful discussions, to Dr. Ger Pruijn for the generous gift of Sm antibodies, and to other members of CEBI for constructive comments and discussions, in particular Drs. Gerhard Mittler and Juri Rappsilber for advice on snRNAs.

Received: August 22, 2003
Revised: March 25, 2004
Accepted: March 29, 2004
Published: May 27, 2004

References

Aebersold, R., and Mann, M. (2003). Mass spectrometry-based proteomics. Nature *422*, 198–207.

Blagoev, B., Kratchmarova, I., Ong, S.E., Nielsen, M., Foster, L.J., and Mann, M. (2003). A proteomics strategy to elucidate functional protein-protein interactions applied to EGF signaling. Nat. Biotechnol. *21*, 315–318.

Buensuceso, C.S., Woodside, D., Huff, J.L., Plopper, G.E., and O'Toole, T.E. (2001). The WD protein Rack1 mediates protein kinase C and integrin-dependent cell migration. J. Cell Sci. *114*, 1691–1698.

Cox, E.A., Bennin, D., Doan, A.T., O'Toole, T., and Huttenlocher, A. (2003). RACK1 regulates integrin-mediated adhesion, protrusion, and chemotactic cell migration via its Src-binding site. Mol. Biol. Cell *14*, 658–669.

Foster, L.J., de Hoog, C.L., and Mann, M. (2003). Unbiased quantita-

tive proteomics of lipid rafts reveals high specificity for signaling factors. Proc. Natl. Acad. Sci. USA *100*, 5813–5818.

Geiger, B., and Bershadsky, A. (2001). Assembly and mechanosensory function of focal contacts. Curr. Opin. Cell Biol. *13*, 584–592.

Habelhah, H., Shah, K., Huang, L., Ostareck-Lederer, A., Burlingame, A.L., Shokat, K.M., Hentze, M.W., and Ronai, Z. (2001). ERK phosphorylation drives cytoplasmic accumulation of hnRNP-K and inhibition of mRNA translation. Nat. Cell Biol. *3*, 325–330.

Huttenlocher, A., Ginsberg, M.H., and Horwitz, A.F. (1996). Modulation of cell migration by integrin-mediated cytoskeletal linkages and ligand-binding affinity. J. Cell Biol. *134*, 1551–1562.

Kambach, C., Walke, S., Young, R., Avis, J.M., de la Fortelle, E., Raker, V.A., Luhrmann, R., Li, J., and Nagai, K. (1999). Crystal structures of two Sm protein complexes and their implications for the assembly of the spliceosomal snRNPs. Cell *96*, 375–387.

Kaverina, I., Krylyshkina, O., and Small, J.V. (2002). Regulation of substrate adhesion dynamics during cell motility. Int. J. Biochem. Cell Biol. *34*, 746–761.

Kislauskis, E.H., Zhu, X., and Singer, R.H. (1997). beta-Actin messenger RNA localization and protein synthesis augment cell motility. J. Cell Biol. *136*, 1263–1270.

Krecic, A.M., and Swanson, M.S. (1999). hnRNP complexes: composition, structure, and function. Curr. Opin. Cell Biol. *11*, 363–371.

Latham, V.M., Yu, E.H., Tullio, A.N., Adelstein, R.S., and Singer, R.H. (2001). A Rho-dependent signaling pathway operating through myosin localizes beta-actin mRNA in fibroblasts. Curr. Biol. *11*, 1010–1016.

Lawrence, J.B., and Singer, R.H. (1986). Intracellular localization of messenger RNAs for cytoskeletal proteins. Cell *45*, 407–415.

Liliental, J., and Chang, D.D. (1998). Rack1, a receptor for activated protein kinase C, interacts with integrin beta subunit. J. Biol. Chem. *273*, 2379–2383.

Meli, M., Albert-Fournier, B., and Maurel, M.C. (2001). Recent findings in the modern RNA world. Int. Microbiol. *4*, 5–11.

Murphy-Ullrich, J.E. (2001). The de-adhesive activity of matricellular proteins: is intermediate cell adhesion an adaptive state? J. Clin. Invest. *107*, 785–790.

Ong, S.E., Blagoev, B., Kratchmarova, I., Kristensen, D.B., Steen, H., Pandey, A., and Mann, M. (2002). Stable isotope labeling by amino acids in cell culture, SILAC, as a simple and accurate approach to expression proteomics. Mol. Cell. Proteomics *1*, 376–386.

Ong, S.E., Foster, L.J., and Mann, M. (2003a). Mass spectrometric-based approaches in quantitative proteomics. Methods *29*, 124–130.

Ong, S.E., Kratchmarova, I., and Mann, M. (2003b). Properties of 13C-substituted arginine in stable isotope labeling by amino acids in cell culture (SILAC). J. Proteome Res. *2*, 173–181.

Orr, A.W., Pedraza, C.E., Pallero, M.A., Elzie, C.A., Goicoechea, S., Strickland, D.K., and Murphy-Ullrich, J.E. (2003). Low density lipoprotein receptor-related protein is a calreticulin coreceptor that signals focal adhesion disassembly. J. Cell Biol. *161*, 1179–1189.

Ostareck-Lederer, A., Ostareck, D.H., Cans, C., Neubauer, G., Bomsztyk, K., Superti-Furga, G., and Hentze, M.W. (2002). c-Src-mediated phosphorylation of hnRNP K drives translational activation of specifically silenced mRNAs. Mol. Cell. Biol. *22*, 4535–4543.

Petit, V., and Thiery, J.P. (2000). Focal adhesions: structure and dynamics. Biol. Cell. *92*, 477–494.

Pickford, A.S., and Cogoni, C. (2003). RNA-mediated gene silencing. Cell. Mol. Life Sci. *60*, 871–882.

Pruijn, G.J., Schoute, F., Thijssen, J.P., Smeenk, R.J., and van Venrooij, W.J. (1997). Mapping of SLE-specific Sm B cell epitopes using murine monoclonal antibodies. J. Autoimmun. *10*, 127–136.

Ranish, J.A., Yi, E.C., Leslie, D.M., Purvine, S.O., Goodlett, D.R., Eng, J., and Aebersold, R. (2003). The study of macromolecular complexes by quantitative proteomics. Nat. Genet. *33*, 349–355.

Ron, D., Chen, C.H., Caldwell, J., Jamieson, L., Orr, E., and Mochly-Rosen, D. (1994). Cloning of an intracellular receptor for protein kinase C: a homolog of the beta subunit of G proteins. Proc. Natl. Acad. Sci. USA *91*, 839–843.

Sastry, S.K., and Burridge, K. (2000). Focal adhesions: a nexus for intracellular signaling and cytoskeletal dynamics. Exp. Cell Res. *261*, 25–36.

Shestakova, E.A., Singer, R.H., and Condeelis, J. (2001). The physiological significance of beta-actin mRNA localization in determining cell polarity and directional motility. Proc. Natl. Acad. Sci. USA *98*, 7045–7050.

Small, J.V., and Kaverina, I. (2003). Microtubules meet substrate adhesions to arrange cell polarity. Curr. Opin. Cell Biol. *15*, 40–47.

Turner, C.E. (2000). Paxillin interactions. J. Cell Sci. *113*, 4139–4140.

Turner, C.E., West, K.A., and Brown, M.C. (2001). Paxillin-ARF GAP signaling and the cytoskeleton. Curr. Opin. Cell Biol. *13*, 593–599.

Wade, R., Bohl, J., and Vande Pol, S. (2002). Paxillin null embryonic stem cells are impaired in cell spreading and tyrosine phosphorylation of focal adhesion kinase. Oncogene *21*, 96–107.

Will, C.L., and Luhrmann, R. (2001). Spliceosomal UsnRNP biogenesis, structure and function. Curr. Opin. Cell Biol. *13*, 290–301.

Woods, A.J., Roberts, M.S., Choudhary, J., Barry, S.T., Mazaki, Y., Sabe, H., Morley, S.J., Critchley, D.R., and Norman, J.C. (2002). Paxillin associates with poly(A)-binding protein 1 at the dense endoplasmic reticulum and the leading edge of migrating cells. J. Biol. Chem. *277*, 6428–6437.

Zamir, E., and Geiger, B. (2001). Molecular complexity and dynamics of cell-matrix adhesions. J. Cell Sci. *114*, 3583–3590.